Scale disparities in the complex Swift-Hohenberg equation for lasers

Carlos Martel[1] and Miguel Hoyuelos[2]
[1]*Departamento de Fundamentos Matemáticos, ETSI Aeronáuticos, Universidad Politécnica de Madrid, 28040 Madrid, Spain*
[2]*Departamento de Física, Facultad de Ciencias Exactas y Naturales, Universidad Nacional de Mar del Plata, Funes 3350, 7600 Mar del Plata, Argentina*

(Received 25 January 2006; revised manuscript received 22 May 2006; published 14 September 2006)

The complex Swift-Hohenberg (CSH) equation is a generic order parameter equation that applies to many physical systems. In the case of class C lasers, it can be obtained from the Maxwell-Bloch equations using the assumptions of slow envelope and small detuning. We show that the resulting CSH equation inevitably contains different asymptotic order terms, associated with the dominance of the effect of dispersion over diffusion. These scale disparities are usually overlooked or simply not mentioned in the literature, assuming that a CSH equation with all terms of the same order still provides qualitative information. In this paper, the asymptotically nonuniform CSH equation is carefully deduced using a simpler scaling-free procedure, and a stability analysis of the simplest solutions together with some numerical simulations are presented, in which the mentioned scale disparities are clearly seen.

DOI: 10.1103/PhysRevE.74.036206 PACS number(s): 05.45.−a, 42.65.Sf

I. INTRODUCTION

Nonlinear optical systems, such as laser, optical parametric oscillator, photorefractive oscillator, or Kerr medium, have been specially prolific during recent decades in providing examples of pattern formation [1–3]. In the case of lasers, there are many experimental confirmations of the presence of transverse patterns. Some of these results are the observation of structures of dotlike localized objects in CO_2 laser [4], phase singularities [5], and patterns in CO_2 and Na_2 lasers [6–8]. It is worth mentioning the observation of transverse patterns in a photorefractive oscillator [9] that was shown to be theoretically equivalent to a class A laser [10]; these patterns are well described by the complex Swift-Hohenberg (CSH) order parameter equation.

Despite the peculiarities of the different classes of lasers, a general theoretical description of transverse patterns in wide aperture single longitudinal mode lasers is obtained from the Maxwell-Bloch equations. These semiclassical equations have been derived and studied by many authors [11–15]. Close to lasing threshold, the description can be greatly simplified through the deduction of a generic order parameter equation whose form depends on the destabilization mechanism and symmetry properties. It has been shown that, when the laser is operating near peak gain (small detuning), such generic description is provided by a CSH equation for class A and C lasers [16,17]. CSH equations for CO_2 laser and semiconductor laser, that are class B, have been obtained in Refs. [18] and [19], respectively. (For an explanation of the classes of lasers, see Ref. [20].) Besides laser and photorefractive oscillators, the CSH equation has been also used as a model for optical parametric oscillators [21,22] and in many other nonoptical contexts [23].

The derivation of the CSH equation from the Maxwell-Bloch equations is based on the slow envelope assumption, i.e., in the assumption that the amplitudes of the physical fields are small and depend slowly on time and on the transversal spatial scales. But the CSH equation is commonly applied without observing the slow envelope requirement and it is not infrequent to see in the literature solutions that do not exhibit only long scales (see Ref. [1] and [3] and the references therein). This is usually justified invoking the argument of a qualitative only scope of the order parameter description.

For the laser parameter values that we will consider, namely class C with small detuning, the resulting CSH equation necessarily includes terms of different asymptotic order and, in some particular regimes, it even allows us to further simplify the CSH equation to a complex Ginzburg-Landau (CGL) equation. This unavoidable asymptotic nonuniformity of the resulting CSH equation is obviated in the usual analysis in the literature, where a CSH equation with all terms of the same order is normally used to analyze this laser instability.

The purpose of this paper is precisely to highlight this point: the correct description of the problem is given by a CSH equation with terms of different asymptotic order. We will write the CSH equation in a way that makes explicit the different magnitudes of each term and will analyze the consequences of these scale disparities in the stability of the most simple solutions. In Sec. II we obtain the CSH equation from the Maxwell-Bloch equations using a method that is simpler than that usually found in the literature, in which no *a priori* relative scaling of the variables is assumed. In Sec. III, the linear and global stability of the nonlasing solution is analyzed. The stability of the traveling waves is studied in Sec. IV, and in Sec. V some numerical simulations of the CSH are presented in order to show the effect of the abovementioned asymptotic nonuniformity. Finally, some concluding remarks are drawn in Sec. VI.

II. THE COMPLEX SWIFT-HOHENBERG EQUATION

The Maxwell-Bloch equations for a two-level single longitudinal mode laser with flat mirrors are

$$\frac{\partial E}{\partial t} = ia\nabla^2 E - \sigma E + \sigma P, \tag{1}$$

$$\frac{\partial P}{\partial t} = -(1+i\Omega)P + (r-N)E, \tag{2}$$

$$\frac{\partial N}{\partial t} = -bN + \frac{1}{2}(\bar{E}P + E\bar{P}). \tag{3}$$

We are using here the same nondimensional formulation as in Ref. [24], where $E(x,y,t)$ and $P(x,y,t)$ represent the complex electric and polarization fields, $N(x,y,t)$ is the real valued field of the population inversion, $a>0$ measures the strength of the diffraction, $\sigma>0$ and Ω account for the cavity losses and the cavity detuning, r is the pumping parameter, $b>0$ is the decay rate of the population inversion, $\nabla^2 = \partial^2/\partial x^2 + \partial^2/\partial y^2$ is the Laplacian operator in the plane transverse to light propagation, and the bar stands for the complex conjugate. In the equations above, the size of the fields have been scaled in order to remove the coefficients of the nonlinear terms and time is measured using the characteristic decay time of the polarization. Note also that the diffraction coefficient, a, can be set to 1 without loss of generality (as we will do hereafter) just by scaling the space variables $\mathbf{x} = (x,y)$ with the diffraction length $\sqrt{a}$. We will consider, as a specific case, a class C laser, for which $\sigma \sim 1$ and $b \sim 1$.

A linear stability analysis of the nonlasing state $(E,P,N)=(0,0,0)$ gives the following stability exponents of small perturbations:

$$\lambda = -b, \tag{4}$$

$$\lambda = -\frac{\sigma+1+i(k^2+\Omega)}{2} \pm \frac{\sqrt{[(\sigma-1)+i(k^2-\Omega)]^2+4r\sigma}}{2}, \tag{5}$$

where k is the absolute value of the perturbation wave number. After some algebra, it is found that the zero solution is stable if the pump, r, is below the critical value $r_c = 1+(k^2-\Omega)^2/(\sigma+1)^2$, and unstable otherwise [16,17]. It is known that, if $\Omega<0$, the Maxwell-Bloch equations can be reduced to a complex Ginzburg-Landau (CGL) equation close to the instability threshold [24], and, if $\Omega>0$, a pair of counterpropagating coupled CGL equations are obtained for 1D and quasi-1D configurations [24–26]. The order parameter equation that completely describes the destabilization in 2D for $\Omega>0$ is not currently known, and it still constitutes one of the open problems in pattern formation [23].

This paper covers the transitional case of small detuning $|\Omega| \ll 1$ in a class C laser, which is described by a CSH equation [16,17].

Near the destabilization threshold, the weakly nonlinear dynamics of the system is dominated by its linear part, and the order of magnitude of the slow scales that the system exhibits can be obtained from the study of the behavior of the stability exponent responsible for the stability change (whose real part first becomes positive as the pump is increased). The small nonlinearities of the problem do not play any role in the slow scale selection; they just define the characteristic size of the resulting pattern through the saturation of the instability growth, and they will be taken into account later on.

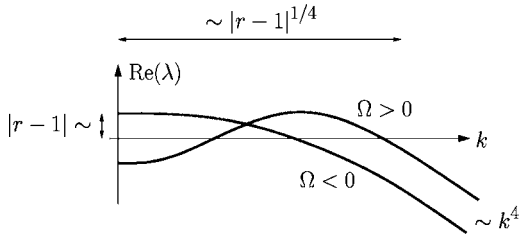

FIG. 1. Sketch of the growth rate of the most unstable modes right after onset, for $|\Omega| \ll 1$, $|r-1| \ll 1$, and $k \ll 1$. The range of almost neutral modes is of order $|r-1|^{1/4}$.

For small detuning, the modes of the system that first become unstable are those corresponding to small wave vectors, and their linear stability characteristics are given by expression (5) with the + sign, which can be expanded as

$$\mathrm{Re}(\lambda) = \frac{\sigma}{\sigma+1}(r-1) - \frac{\sigma}{(\sigma+1)^3}(k^2-\Omega)^2 + \cdots, \tag{6}$$

$$\mathrm{Im}(\lambda) = -\frac{k^2+\sigma\Omega}{\sigma+1} + \cdots, \tag{7}$$

in the limit of small detuning, small displacement from threshold, and small wave vector, i.e.,

$$|\Omega| \ll 1, \quad |r-1| \ll 1 \quad \text{and } k \ll 1. \tag{8}$$

From the expression of the growth rate (6), we can see that the characteristic slow time is given by $\tau \sim 1/|r-1| \gg 1$ and that the range of almost neutral modes goes up to $k \sim |r-1|^{1/4}$ (see Fig. 1). The growth rate of the modes with $k \gg |r-1|^{1/4}$ is much larger and negative and therefore they are quickly damped out in the slow time scale. Note that in the scaling arguments above we are implicitly assuming that $|\Omega|$ is, at most, of the order of $|r-1|^{1/2}$. We are not considering the case $|\Omega| \gg |r-1|^{1/2}$ and $\Omega>0$ ($\Omega<0$ is stable and far from threshold, see Ref. [24]), in which a narrow band of almost neutral modes of size $\Delta k \sim |r-1|^{1/2}/\sqrt{|\Omega|}$ develops around the critical wave-vector circumference of radius $k_c \sim \sqrt{|\Omega|} \gg \Delta k$, because it corresponds to a completely different destabilization type for which, as mentioned before, a couple of counterpropagating CGL equations are obtained in 1D systems.

In other words, the behavior of the growth rate ensures that, for large times, the system can only exhibit spatial scales that are of the order $1/|r-1|^{1/4} \gg 1$ or larger, but no smaller ones, because those are damped out by the dominant linear effects.

On the other hand, the associated mode frequencies given by Eq. (7) are always large as compared with the damping terms of the growth rate. This indicates that the effect of dispersion on the neutral modes of the system is faster and much stronger than that of diffusion. The envelope equation that describes the slow dynamics of the system has to take into account these two effects simultaneously and therefore it is necessarily going to contain terms of different asymptotic

orders, which can never be rescaled to be of the same order. This is not the case in the transition for $\Omega<0$, where dispersion and diffusion are both of the same order $\sim k^2$ and the weakly nonlinear dynamics of the system is described by an asymptotically uniform complex Ginzburg-Landau equation [24].

The need to retain terms of different orders made the derivation of the envelope equation in Refs. [16] and [17] quite involved. They first assumed a particular scaling for the fields and the slow spatial and temporal variables, then they proceeded to derive the envelope equation and its next order correction, and, finally, they collapsed back the two term expansion into the original (unscaled) variables in order to obtain a single envelope equation.

The derivation of the envelope equation that we present below is simpler because we do not assume *a priori* any scaling relation between the variables, we just look for small-amplitude solutions that depend slowly on space and time (similar scaling-free derivations can be found in Refs. [27] and [28] in the context of convection and water waves).

More precisely, the neutral mode at threshold, $r=1$ and $\Omega=0$, corresponds to $\lambda=0$ and $k=0$, with associated eigenvector

$$V_0=\begin{bmatrix}1\\1\\0\end{bmatrix},$$

and suggests an expansion for the solution of the MB equations (1)–(3) of the form

$$\begin{bmatrix}E(x,y,t)\\P(x,y,t)\\N(x,y,t)\end{bmatrix}=V_0\psi+V_1\nabla^2\psi+\cdots, \tag{9}$$

where the complex amplitude $\psi(x,y,t)$ has to verify a solvability condition that is also expanded as

$$\psi_t=\alpha_0\psi+\alpha_1\nabla^2\psi+\cdots, \tag{10}$$

and is precisely the envelope equation that we are looking for. The expansions above include all possible combined powers of the small quantities

$$|\Omega|\ll 1,\quad |r-1|\ll 1,\quad \text{and } |\psi|\ll 1,|\nabla^2\psi|\ll 1,|\nabla^4\psi|\ll 1,\ldots$$

that are treated as independent parameters, only constrained by the weakly nonlinear level of this approach, which requires essentially that

$$\cdots\ll|\nabla^4\psi|\ll|\nabla^2\psi|\ll|\psi|\ll 1 \text{ and } \cdots\ll|\psi_t|\ll|\psi|\ll 1\ldots,$$

i.e., small envelope amplitude and slow time and space dependence (we have also anticipated the fact that only even order spatial derivatives will be produced because of the symmetry $\mathbf{x}\to-\mathbf{x}$ of the system).

When the above expansions (9) and (10) are inserted in the MB equations (1)–(3), a linear nonhomogeneous singular system is obtained at each order. And, as it is the standard procedure in multiple scale methods to ensure that no secular terms are present [29,30], the nonhomogeneous terms of these systems must satisfy a solvability condition that provides the contribution of this order to the envelope equation.

The linear terms of the envelope equation (10) can be easily anticipated because they correspond to the Taylor expansion of the critical eigenvalue branch $\lambda(k^2,r,\Omega)$ [Eq. (5) with the + sign] at $(k^2,r,\Omega)=(0,1,0)$ (see, e.g., Ref. [23]),

$$\lambda_{(0,1,0)}\psi+\left.\frac{\partial\lambda}{\partial r}\right|_{(0,1,0)}(r-1)\psi+\left.\frac{\partial\lambda}{\partial\Omega}\right|_{(0,1,0)}\Omega\psi-\left.\frac{\partial\lambda}{\partial(k^2)}\right|_{(0,1,0)}\nabla^2\psi+\frac{1}{2}\left.\frac{\partial^2\lambda}{\partial(k^2)^2}\right|_{(0,1,0)}\nabla^4\psi-\left.\frac{\partial^2\lambda}{\partial\Omega\partial(k^2)}\right|_{(0,1,0)}\Omega\nabla^2\psi+\frac{1}{2}\left.\frac{\partial^2\lambda}{\partial\Omega^2}\right|_{(0,1,0)}\Omega^2\psi+\cdots,$$

and thus, according to expressions (6) and (7), are of the form

$$\frac{\sigma}{\sigma+1}[(r-1)-i\Omega]\psi+i\frac{1}{(\sigma+1)}\nabla^2\psi-\frac{\sigma}{(\sigma+1)^3}(\Omega+\nabla^2)^2\psi+\cdots. \tag{11}$$

The computation of the nonlinear terms requires us to take the expansions (9) and (10) to the MB equations, which should be first rewritten in the more convenient form

$$\begin{bmatrix}\sigma&-\sigma&0\\-1&1&0\\0&0&b\end{bmatrix}\begin{bmatrix}E\\P\\N\end{bmatrix}=-\frac{\partial}{\partial t}\begin{bmatrix}E\\P\\N\end{bmatrix}+\begin{bmatrix}i\nabla^2E\\(r-1)E-i\Omega P\\0\end{bmatrix}+\begin{bmatrix}0\\-NE\\\frac{1}{2}(\bar{E}P+E\bar{P})\end{bmatrix}, \tag{12}$$

with the dominant terms grouped on the left-hand side. The first-order nonlinear contribution to the expansions (9) and (10) is given by

$$V|\psi|^2 \text{ and } \alpha|\psi|^2,$$

where the vector V and the scalar α are obtained from

$$\begin{bmatrix}\sigma&-\sigma&0\\-1&1&0\\0&0&b\end{bmatrix}V=-\alpha V_0+\begin{bmatrix}0\\0\\1\end{bmatrix}.$$

This singular linear system can only be solved if the right-hand side is orthogonal to the solution of the adjoint problem

$$V_0^a=\begin{bmatrix}1\\\sigma\\0\end{bmatrix},$$

and this solvability condition yields

$$V = \begin{bmatrix} 0 \\ 0 \\ \frac{1}{b} \end{bmatrix} \text{ and } \alpha = 0.$$

Thus there is no contribution of this term to the envelope equations, in other words, it is not a resonant term. At next order we have the terms

$$W\psi|\psi|^2 \text{ and } \beta\psi|\psi|^2,$$

which must verify

$$\begin{bmatrix} \sigma & -\sigma & 0 \\ -1 & 1 & 0 \\ 0 & 0 & b \end{bmatrix} W = -\beta V_0 + \begin{bmatrix} 0 \\ -\frac{1}{b} \\ 0 \end{bmatrix},$$

and, again, we apply the solvability condition to obtain the following coefficient of the envelope equation:

$$\beta = -\frac{\sigma}{b(1+\sigma)}.$$

Finally, after collecting the leading nonlinear contribution above and the linear terms in Eq. (11), the envelope equation reads

$$\psi_t = \frac{\sigma[(r-1)-i\Omega]}{\sigma+1}\psi + \frac{i}{(\sigma+1)}\nabla^2\psi - \frac{\sigma}{(\sigma+1)^3}(\Omega+\nabla^2)^2\psi - \frac{\sigma}{b(\sigma+1)}\psi|\psi|^2 + \cdots, \quad (13)$$

which is the well known complex Swift-Hohenberg equation (CSH) (see Refs [16] and [17]). It is important to stress that this equation has to be solved in the limit

$$|\Omega| \ll 1 \text{ and } |r-1| \ll 1, \quad (14)$$

and that its solutions must verify the slow envelope assumption

$$\cdots \ll |\nabla^4\psi| \ll |\nabla^2\psi| \ll |\psi| \ll 1. \quad (15)$$

And therefore, as was expected from the study of the growth rate, the CSH above contains different order terms: the effect of dispersion is always much bigger than the dissipation of the double diffusive term.

We now introduce the small parameter $0 < \varepsilon \ll 1$ and the scaling of the variables,

$$(r-1) - \frac{\Omega^2}{(\sigma+1)^2} = \frac{(\sigma+1)^2}{\sigma^2}\alpha\varepsilon^2, \quad \tilde{t} = \frac{(\sigma+1)}{\sigma}t\varepsilon^2,$$

$$(\tilde{x},\tilde{y}) = \frac{(\sigma+1)}{\sqrt{\sigma}}(x,y)\varepsilon, \quad \psi = e^{-i[\sigma\Omega/(\sigma+1)]t}\sqrt{b}\frac{(\sigma+1)}{\sigma}\phi\varepsilon,$$

$$\Omega = \frac{(\sigma+1)^2}{\sigma}\omega\varepsilon, \quad (16)$$

which brings Eq. (13), after dropping tildes, to the more convenient form

$$\phi_t = \alpha\phi + i\nabla^2\phi - \phi|\phi|^2 - 2\varepsilon\omega\nabla^2\phi - \varepsilon^2\nabla^4\phi, \quad (17)$$

where the rescaled pump, α, and detuning, ω, are now order 1 parameters.

In the scaled CSH Eq. (17), the dominant dispersion induced dynamics is of order 1: the typical length scale exhibited by the dispersive patterns (that was $\sim 1/\sqrt{|r-1|} \gg 1$ in the original variables) is now $\delta_{\text{disp}} \sim 1$. On the other hand, the small coefficient multiplying the double diffusive term indicates that the system is capable of displaying scales as small as $\delta_{\text{diff}} \sim \sqrt{\varepsilon}$ ($\sim 1/\sqrt[4]{|r-1|} \gg 1$ in the original variables) before diffusion becomes overwhelming and everything is damped out, recall Fig. 1.

The simplest solutions of Eq. (17) are those that only exhibit scales $\sim \delta_{\text{disp}} \sim 1$ as $\varepsilon \to 0$. For those dispersive states, the spatial derivatives remain of order 1 and thus the two last terms in Eq. (17) represent, in the limit $\varepsilon \to 0$, a small correction that can be neglected to give

$$\phi_t = \alpha\phi + i\nabla^2\phi - \phi|\phi|^2. \quad (18)$$

This is a very interesting complex Ginzburg-Landau equation (CGL) [23,31,32]: purely dispersive but with a dissipation that comes from the nonlinear term only. This CGL equation appears in a straightforward way from the small detuning MB equations due to the dominant character of the dispersion, but, so far, we have not seen it analyzed in the literature. Instead, the equations that are currently used to describe the weakly nonlinear dynamics of the MB equations in the small detuning case are either (i) the unscaled CSH Eq. (13), but integrated without observing the slow envelope, near threshold conditions (14) and (15), see Refs. [16,17,24], and [33], or (ii) a CSH equation scaled similarly to Eq. (17), see Ref. [34], but again studied for $\varepsilon \sim 1$, when $\varepsilon \ll 1$ is the only physically relevant regime from the point of view of the slow envelope description of the transverse laser pattern dynamics.

The next sections are dedicated to the study of some basic solutions of Eq. (18). Note that once a stable solution of Eq. (18) is found, in order to be sure that it is a stable state of the complete CSH Eq. (17), one must also check its stability under perturbations containing small diffusive scales, whose dynamics is not contained in Eq. (18); and if the small diffusive scales are not damped out, then the complete CSH Eq. (17) with $\varepsilon \to 0$ has to be used in order to correctly describe the dynamics of the system.

III. LINEAR AND GLOBAL STABILITY OF THE NONLASING SOLUTION

In this section, we study the stability properties of the nonlasing solution $\phi = 0$. We are interested in the bulk behavior of a big extended system, where the boundary conditions do not play a relevant role. The simplest choice is a periodic boundary condition in a square domain, and the solutions of the linearized version of the CSH equation in this case can be written in the form

$$\phi \sim e^{i\mathbf{k}\cdot\mathbf{x}+\lambda t},$$

where λ is given by

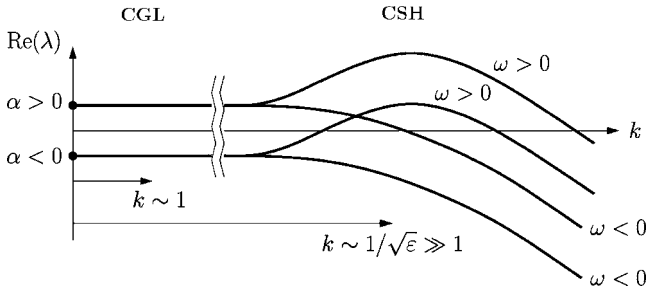

FIG. 2. Growth rate of the perturbations of the zero solution of the CSH Eq. (17) for $\omega>0$ and $\omega<0$, with the two wave-number regions shown: $k\sim 1$ (dispersive perturbations, $\delta_{\text{disp}}\sim 1$) and $k\sim 1/\sqrt{\varepsilon}\gg 1$ (diffusive perturbations, $\delta_{\text{diff}}\sim\sqrt{\varepsilon}$). This plot is a rescaled version of Fig. 1, obtained after the variable changes of Eq. (16), where the regimes dominated by the CGL and CSH equations are distinguished.

$$\lambda = \alpha - ik^2 + 2\varepsilon\omega k^2 - \varepsilon^2 k^4,$$

with $k=|\mathbf{k}|$ and $0<\varepsilon\ll 1$. Two different kinds of perturbations can be distinguished. The first are those with wave vector $k\sim 1$, i.e., those exhibiting only dispersive scales $\delta_{\text{disp}}\sim 1$, for which the dispersion relation above simplifies to

$$\lambda = \alpha - ik^2 + \cdots, \tag{19}$$

and thus are stable for $\alpha<0$ and become unstable for $\alpha>0$. The evolution of these perturbations is well represented by the CGL, which could have been used to obtain their stability properties. The second kind of perturbations are those with very high wave vector $k\sim K/\sqrt{\varepsilon}\gg 1$ and $K\sim 1$, which have a typical wavelength of the order of the small diffusive scales $\delta_{\text{diff}}\sim\sqrt{\varepsilon}\ll 1$, and whose growth rate is given by

$$\text{Re}(\lambda) = \alpha + 2\omega K^2 - K^4.$$

For negative detuning $\omega<0$ these small-scale perturbations become unstable for positive α, but for $\omega>0$ the destabilization takes place for $\alpha>-\omega^2$ at a critical wave number $k=\sqrt{\omega}/\sqrt{\varepsilon}\gg 1$. The dynamics of these perturbations is not included in the CGL and its analysis requires us to deal with the complete CSH.

The structure of the growth rate of these perturbations is sketched in Fig. 2 and, as was expected, it is just a rescaled version of that obtained in the previous section for the MB, see Fig. 1. The resulting stability region of the nonlasing solution is the dark shaded area in the $\alpha-\omega$ plot in Fig. 3.

Inside the linear stability region indicated with dark shading in Fig. 3, the zero solution is, in fact, globally stable, that is, all solutions of the CSH for all possible initial conditions decay to 0 as time increases. In order to see this, we multiply Eq. (17) by $\bar{\phi}$, add the complex conjugate, and integrate over the domain D to obtain

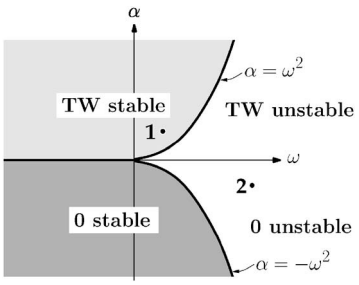

FIG. 3. Stability diagram for the zero solution and the TW. Light shading: TW stable. Dark shading: zero solution stable. The axes correspond to the scaled pump α, and detuning ω, that are quantities of order 1. Numbered dots indicate the parameter values used in the numerical simulations in Sec. V.

$$\frac{d}{dt}\int_D |\phi|^2 = 2\int_D |\phi|^2(\alpha - |\phi|^2) + i\int_D (\bar{\phi}\nabla^2\phi - \phi\nabla^2\bar{\phi}) - 2\varepsilon\omega\int_D (\bar{\phi}\nabla^2\phi + \phi\nabla^2\bar{\phi}) + \varepsilon^2\int_D (\bar{\phi}\nabla^4\phi + \phi\nabla^4\bar{\phi}).$$

If we now take into account that

$$\bar{\phi}\nabla^2\phi = \nabla\cdot(\bar{\phi}\,\nabla\,\phi) - |\nabla\phi|^2,$$

and apply Green's formula, the second integral above can be expressed as

$$\int_D \nabla\cdot(\bar{\phi}\,\nabla\,\phi - \phi\,\nabla\,\bar{\phi}) = \int_{\delta D}\left(\bar{\phi}\frac{\partial\phi}{\partial n} - \phi\frac{\partial\bar{\phi}}{\partial n}\right) = 0,$$

which is zero because of the periodicity boundary conditions at the boundary δD of the square domain D. The same arguments allow us to write

$$\int_D (\bar{\phi}\nabla^2\phi + \phi\nabla^2\bar{\phi}) = -2\int_D |\nabla\phi|^2$$

and

$$\int_D (\bar{\phi}\nabla^4\phi + \phi\nabla^4\bar{\phi}) = 2\int_D |\nabla^2\phi|^2,$$

where we have also made use of the relation

$$\bar{\phi}\nabla^4\phi = \nabla\cdot[\bar{\phi}\,\nabla\,(\nabla^2\phi) - (\nabla\bar{\phi})(\nabla^2\phi)] + |\nabla^2\phi|^2.$$

And collecting all the above results, one can write

$$\frac{d}{dt}\int_D |\phi|^2 = 2\left[\int_D |\phi|^2(\alpha - |\phi|^2) + 2\varepsilon\omega\int_D |\nabla\phi|^2 - \varepsilon^2\int_D |\nabla^2\phi|^2\right] \tag{20}$$

and also

$$\frac{d}{dt}\int_D |\phi|^2 = 2\left[\int_D |\phi|^2(\alpha+\omega^2-|\phi|^2) - \int_D |\varepsilon\nabla^2\phi+\omega\phi|^2\right], \tag{21}$$

as it can be readily seen after taking into account the following relation:

$$|\varepsilon\nabla^2\phi+\omega\phi|^2 = \varepsilon^2|\nabla^2\phi|^2+\omega^2|\phi|^2+\varepsilon\omega(\bar{\phi}\nabla^2\phi+\phi\nabla^2\bar{\phi})$$

and the result above for the integral of its last term.

Finally, for $\omega<0$ all negative terms on the right-hand side of Eq. (20) can be removed to give

$$\frac{d}{dt}\int_D |\phi|^2 \leqslant 2\alpha\int_D |\phi|^2,$$

which, according to Gronwall's Lemma, implies that

$$\int_D |\phi|^2 \leqslant Ce^{2\alpha t} \to 0 \quad \text{as } t\to\infty,$$

and thus we can conclude that

$$\int_D |\phi|^2 \to 0 \quad \text{as } t\to\infty,$$

i.e., all solutions decay to zero for $\alpha<0$ and $\omega<0$. If now $\omega>0$, then we can use Eq. (21) and follow the same argumentation as above to obtain that, for $\alpha+\omega^2<0$, all solutions also decay to zero.

IV. TRAVELING WAVE SOLUTIONS

The simplest nonzero solutions of the CGL Eq. (18) are the spatially uniform traveling waves (TW),

$$\phi_{\mathrm{TW}} = \sqrt{\alpha}e^{i\mathbf{k}_{\mathrm{TW}}\cdot\mathbf{x}-ik_{\mathrm{TW}}^2 t}, \tag{22}$$

with $k_{\mathrm{TW}}=|\mathbf{k}_{\mathrm{TW}}|\sim 1$, which exist only for $\alpha>0$ and are approximate solutions of the CSH up to $O(\varepsilon)$ corrections.

The TW stability characteristics can be easily obtained looking for solutions of the form

$$\phi = \phi_{\mathrm{TW}}(1+\xi) \quad \text{with } |\xi| \ll 1$$

in the CSH and neglecting all but the linear terms. The following equation for the evolution of the perturbation ξ is obtained:

$$\xi_t = i(\nabla^2\xi + i2\mathbf{k}_{\mathrm{TW}}\cdot\boldsymbol{\nabla}\xi) - \alpha(\xi+\bar{\xi}) - 2\varepsilon\omega[\nabla^2\xi+\cdots] - \varepsilon^2[\nabla^4\xi+\cdots],$$

where, as we will see below, only the main contribution of the small diffusive terms needs to be retained. If we now expand ξ in Fourier series,

$$\xi = \sum \xi_{\mathbf{k}}(t)e^{i\mathbf{k}\cdot\mathbf{x}},$$

only the mode pairs with wave vectors $\pm\mathbf{k}$ are coupled and their evolution equations read

$$\frac{d\xi_{\mathbf{k}}}{dt} = (-\alpha - ik^2 - i2\mathbf{k}_{\mathrm{TW}}\cdot\mathbf{k} + 2\varepsilon\omega k^2 - \varepsilon^2k^4)\xi_{\mathbf{k}} - \alpha\bar{\xi}_{-\mathbf{k}},$$

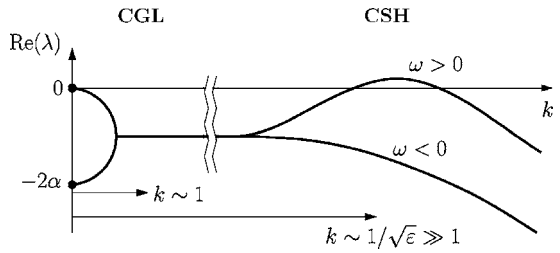

FIG. 4. Growth rate of the perturbations of the TW for $\omega>0$ and $\omega<0$, with the two wave-number regions shown: $k\sim 1$ (dispersive perturbations) and $k\sim 1/\sqrt{\varepsilon}\gg 1$ (diffusive perturbations).

$$\frac{d\bar{\xi}_{-\mathbf{k}}}{dt} = (-\alpha + ik^2 - i2\mathbf{k}_{\mathrm{TW}}\cdot\mathbf{k} + 2\varepsilon\omega k^2 - \varepsilon^2k^4)\bar{\xi}_{-\mathbf{k}} - \alpha\xi_{\mathbf{k}},$$

where $k=|\mathbf{k}|$. The solutions of this linear system are proportional to $e^{\lambda t}$ with λ given by

$$\lambda = -\alpha - i2\mathbf{k}_{\mathrm{TW}}\cdot\mathbf{k} + 2\varepsilon\omega k^2 - \varepsilon^2k^4 \pm \sqrt{\alpha^2-k^4}.$$

Again, we can distinguish between perturbations exhibiting only dispersive scales, i.e., with wave vector $|\mathbf{k}|\sim 1$, which have a growth rate that can be approximated as

$$\mathrm{Re}(\lambda) = -\alpha \pm \sqrt{\alpha^2-k^4} + \cdots \tag{23}$$

and are always stable because α is positive for all TW (see Fig. 4). This is again the result that is obtained if the linear stability analysis is performed on the CGL. And perturbations with high diffusive wave vectors, $k\sim K/\sqrt{\varepsilon}\gg 1$, whose dynamics is not contained in the CGL, and their growth rate, up to $O(\sqrt{\varepsilon})$ corrections, are given by

$$\mathrm{Re}(\lambda) = -\alpha + 2\omega K^2 - K^4 + \cdots, \tag{24}$$

which is also plotted in Fig. 4. These diffusive, short wave perturbations become unstable outside the region defined by $\omega>0$ and $\alpha>\omega^2$ (marked with light shading in Fig. 3) with critical wave number $k=\sqrt{\omega}/\sqrt{\varepsilon}\gg 1$. Note that the growth rate of the diffusive perturbations is of order 1 and thus this is not a higher-order correction that evolves on a much slower time scale; this instability develops in the time scale $t\sim 1$ of the dispersive CGL dynamics.

V. NUMERICAL RESULTS

In this section we present some numerical simulations of the CSH equation (17) in a square domain $[0,1]\times[0,1]$ with periodic boundary conditions. The CSH is integrated in Fourier space using a fourth-order Runge-Kutta scheme, with 64×64 and 128×128 Fourier modes and with a time step in the range $dt=0.001\cdots 0.0001$.

This simulations are performed in order to confirm that, as it was advanced in Sec. II, there are two types of solutions of the CSH with a completely different behavior in the physically relevant limit of large systems $\varepsilon\to 0$: those that only exhibit scales that are of the order of the total size of the domain, $\delta_{\mathrm{disp}}\sim 1$, and that can be accurately approximated by the simpler CGL that is obtained by setting $\varepsilon=0$ in the CSH (case 1 below), and those that develop small diffusive

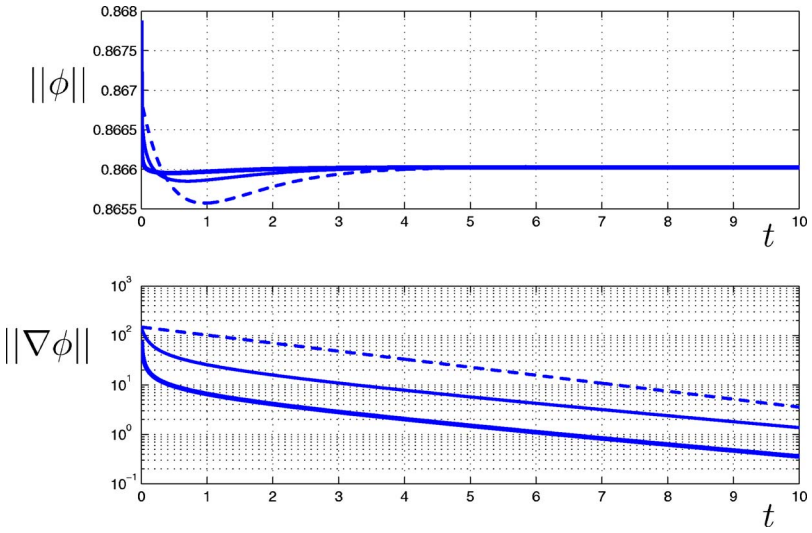

FIG. 5. (Color online) Time evolution of the norm of the solution of the CSH Eq. (17) (above) and its gradient (below). The initial condition is a spatially uniform steady solution with a random perturbation of size 10^{-3}, and the parameters correspond to the case 1 in Fig. 3 with $\varepsilon=10^{-3}$ (thick line), $\varepsilon=10^{-3}/4$ (thin line), and $\varepsilon=0$ [CGL Eq. (18) dashed line].

scales, $\delta_{\text{diff}}\sim\sqrt{\varepsilon}$, whose dynamics can only be correctly described using the asymptotically nonuniform CSH with $\varepsilon \ll 1$ (case 2).

Case 1. $\alpha=0.75$ and $\omega=0.5$. We are in the region of the parameter space where the uniform TWs described by expression (22) in Sec. IV are all stable (see Fig. 3). Recall that these are TWs with wave number $k\sim 1$ (without diffusive scales) and therefore, in the $\varepsilon \ll 1$ limit, they are approximately given by the CGL equation (18). The starting point of the numerical integrations shown in Fig. 5 is now a uniform TW [i.e., that with $\mathbf{k}_{\text{TW}}=(0,0)$ and amplitude $\sqrt{\alpha}$] with a 10^{-3} random perturbation, and, as expected, the system relaxes to the uniform TW: $\|\phi\|\to\sqrt{\alpha}$ and $\|\nabla\phi\|\to 0$. It is interesting to notice that the decay rate for $\varepsilon \ll 1$ appears to be independent of ε (see the slopes of the two solid lines in the lower plot in Fig. 5) but different from that for $\varepsilon=0$ (dashed line in the lower plot in Fig. 5), which decays faster. This is also in agreement with the results from the previous section: the dispersion relation of the TW for $\varepsilon \ll 1$ is given by Eq. (24), whose maximum value $-\alpha+\omega^2=-0.5$ (associated to the slowest decaying modes) is independent of ε and different from that corresponding to $\varepsilon=0$ [when the CSH equation simplifies to the CGL equation (18)] that, according to Eq. (23), is constant and equal to $-\alpha=-0.75$, and thus produces a faster decay to zero.

Case 2. $\alpha=-0.5$ and $\omega=2$. The initial condition is the same perturbed uniform state used in case 1, but now, as is clear from Fig. 6, the behavior of the system for $\varepsilon \ll 1$ is completely different from that for $\varepsilon=0$. The resulting temporal evolution for $\varepsilon=0$ is just a monotonous decay to the zero solution (dashed line in Fig. 6) that, according to Eq. (19), is always stable in the CGL dynamics when α is negative. On the other hand, the zero solution is unstable for the CSH with $\varepsilon \ll 1$ (see Fig. 3), and what happens now is that the system evolves to a nonzero final state that exhibits small diffusive scales (solid lines in Fig. 6). These small diffusive scales grow exponentially with a finite nonzero growth rate as $\varepsilon \to 0$, see the lower plot of Fig. 6. Note that, despite of the small coefficients of diffusion and double diffusion in the CSH Eq. (17), the onset of these small diffusive scales is not a higher-order, longer time scale effect; they evolve in the $t\sim 1$ time scale of the CSH, as is clear from the slope of the solid lines in the lower plot of Fig. 6. The resulting values of $\|\nabla\phi\|$ at $t=20$ for $\varepsilon=10^{-3}$ and $\varepsilon=10^{-3}/4$ are, respectively, 82.187 and 164.85, whose ratio is equal to 2.006…, in agreement with the fact that the small diffusive scales dominate the final state, forcing the norm of the gradient to behave, in

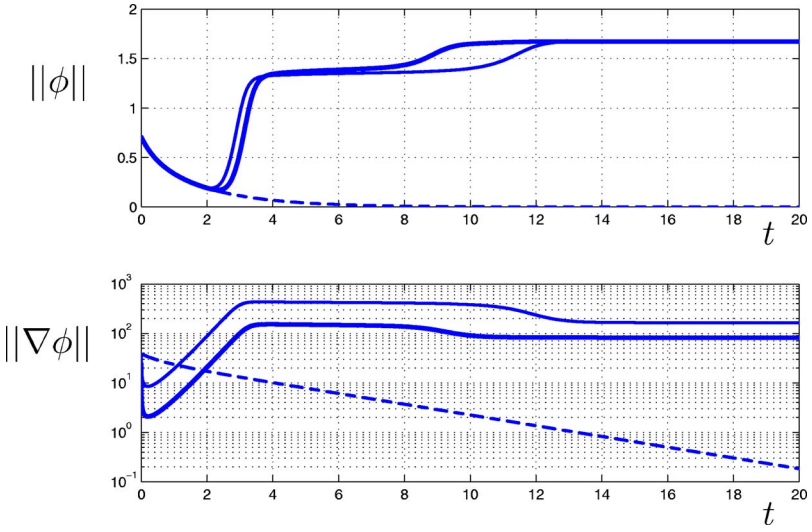

FIG. 6. (Color online) Time evolution of the norm of the solution of the CSH Eq. (17) (above) and its gradient (below). The initial condition is a spatially uniform steady solution with a random perturbation of size 10^{-3}, and the parameters correspond to the case 2 in Fig. 3 with $\varepsilon=10^{-3}$ (thick line), $\varepsilon=10^{-3}/4$ (thin line), and $\varepsilon=0$ [CGL Eq. (18), dashed line].

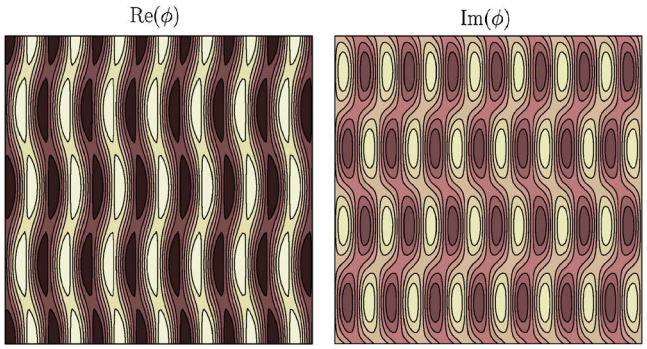

FIG. 7. (Color online) Colored contour maps of the real (left) and imaginary (right) part of the solution of the CSH Eq. (17) at $t=20$ for $\alpha=-0.5$, $\omega=2$, and $\varepsilon=10^{-3}$.

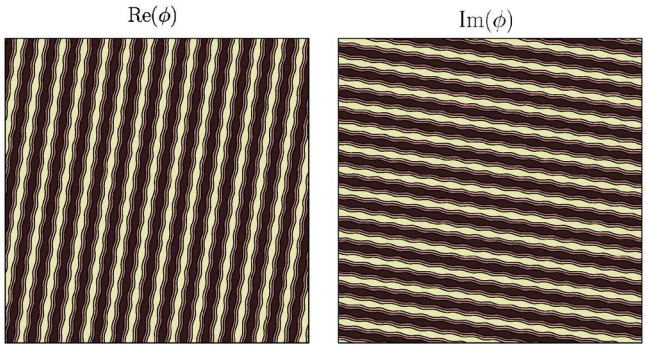

FIG. 8. (Color online) Colored contour maps of the real (left) and imaginary (right) part of the solution of the CSH Eq. (17) at $t=20$ for $\alpha=-0.5$, $\omega=2$, and $\varepsilon=10^{-3}/4$.

first approximation, as $\|\nabla\phi\| \sim 1/\sqrt{\varepsilon}$. Moreover, the solutions at $t=20$ for $\varepsilon=10^{-3}$ and $\varepsilon=10^{-3}/4$ (shown in Figs. 7 and 8) resemble a TW with a number of wavelengths that is roughly 7 and 14, indicating that this final state is close to a TW but with a diffusive wave number $k \sim 1/\sqrt{\varepsilon}$.

VI. CONCLUSIONS

Although the system here analyzed is a specific class C laser at peak gain (or small detuning), the problem of scale disparities in the complex Swift-Hohenberg equation is much more general and involves many different physical systems [23]. The condition assumed for the derivation of the order parameter equation is that the amplitudes of the physical fields are small and depend slowly on time and space. This, inevitably, leads to the presence of terms with different asymptotic order in the CSH equation and to the fact that the small parameter ε cannot be removed from the amplitude equation, which must be solved in the limit $\varepsilon \to 0$. The solutions obtained from a CSH equation with all terms of the same order are not valid in principle because they violate the slow envelope assumption that is precisely the starting point assumption for the derivation of the CSH.

We have deduced the corresponding asymptotically nonuniform CSH equation using a scaling-free method, much simpler than that presented in Refs. [16] and [17]. The resulting CSH is actually a purely dispersive CGL equation plus smaller order diffusion and double diffusion terms, which presents two well defined, extremely different scales: dispersive scales, $\delta_{\text{disp}} \sim 1$, and smaller diffusive scales, $\delta_{\text{diff}} \sim \sqrt{\varepsilon}$ [with the scaling of Eq. (17)].

This scale separation suggests the following procedure: solutions of the simpler CGL equation (that only exhibit dispersive scales) are easily obtained and then their stability is analyzed in the context of the complete CSH equation, where the behavior of the perturbations is also affected by the diffusion and double diffusion terms (whose effect is not necessarily small). The result is that the perturbations of the simplest solutions (nonlasing state and traveling waves) have two different regimes. One regime holds for small perturbation wave number, $k \sim 1$ (dispersive perturbations), and is dominated by the CGL equation. The other regime holds for big wave number, $k \sim 1/\sqrt{\varepsilon}$ (diffusive perturbations), and requires us to consider the complete CSH equation (Figs. 2 and 4). The diagram of Fig. 3 in the parameter space determined by the scaled pump α and detuning ω, which gives the stability regions of the nonlasing and TW solutions, does not depend on the small parameter ε, as $\varepsilon \to 0$. But the perturbations that become unstable when crossing the curves $\alpha=\omega^2$ for TW or $\alpha=-\omega^2$ for the nonlasing state do have a diffusive wave number that does depend on ε and, in both cases, scales as $1/\sqrt{\varepsilon}$.

In summary, we have obtained an asymptotically nonuniform CSH equation for the description of the weakly nonlinear dynamics of a class C laser at peak gain starting from the Maxwell-Bloch equations. In some cases, it can be reduced to a purely dispersive CGL equation. And the presence of dispersive (CGL) and diffusive (CSH) regimes, that were not previously identified, is manifested in the stability analysis of the nonlasing state and traveling waves, and has been confirmed with numerical simulations of the CSH.

ACKNOWLEDGMENTS

This work has been supported by AECI (Agencia Española de Cooperación Internacional), Spain, under Grant No. PCI A/3153/05. M.H. acknowledges COCINET (Consejo Nacional de Investigaciones Científicas y Tecnológicas), Argentina, for partial support. The work of C.M. has been supported by the Spanish Ministerio de Educación y Ciencia under Grant No. MTM2004-03808 and by the European Office of Aerospace Research and Development under Grant No. FA8655-05-1-3040.

[1] F. Arecchi and S. B. P. Ramazza, Phys. Rep. **318**, 1 (1999).
[2] L. Lugiato, M. Brambilla, and A. Gatti, Adv. At., Mol., Opt. Phys. **40**, 229 (1999).
[3] K. Staliunas and V. Sánchez-Morcillo, *Transverse Patterns in Nonlinear Optical Resonators*, Springer Tracts in Modern Physics (Springer-Verlag, Berlin, 2003).
[4] D. Dangoisse, D. Hennequin, C. Lepers, E. Louvergneaux, and P. Glorieux, Phys. Rev. A **46**, 5955 (1992).
[5] N. R. Heckenberg, R. McDuff, C. Smith, H. Rubinsztein-Dunlop, and M. Wegener, Opt. Quantum Electron. **24**, S951 (1992).
[6] E. J. D'Angelo, E. Izaguirre, G. B. Mindlin, G. Huyet, L. Gil, and J. R. Tredicce, Phys. Rev. Lett. **68**, 3702 (1992).
[7] A. B. Coates, C. O. Weiss, C. Green, E. J. D'Angelo, J. R. Tredicce, M. Brambilla, M. Cattaneo, L. A. Lugiato, R. Pirovano, F. Prati, A. J. Kent, and G. L. Oppo, Phys. Rev. A **49**, 1452 (1994).
[8] G. Lippi, H. Grassi, T. Ackemann, A. Aumann, B. Schäpers, J. Seipenbusch, and J. Tredicce, J. Opt. B: Quantum Semiclassical Opt. **1**, 161 (1999).
[9] K. Staliunas, G. Slekys, and C. O. Weiss, Phys. Rev. Lett. **79**, 2658 (1997).
[10] K. Staliunas, M. F. H. Tarroja, G. Slekys, C. O. Weiss, and L. Dambly, Phys. Rev. A **51**, 4140 (1995).
[11] H. Risken and K. Nummedal, J. Appl. Phys. **39**, 4662 (1968).
[12] L. M. Narducci, J. R. Tredicce, L. A. Lugiato, N. B. Abraham, and D. K. Bandy, Phys. Rev. A **33**, 1842 (1986).
[13] L. Lugiato, C. Oldano, and L. Narducci, J. Opt. Soc. Am. B **5**, 879 (1988).
[14] P. Coullet, L. Gil, and F. Rocca, Opt. Commun. **73**, 403 (1989).
[15] P. K. Jakobsen, J. V. Moloney, A. C. Newell, and R. Indik, Phys. Rev. A **45**, 8129 (1992).
[16] J. Lega, J. V. Moloney, and A. C. Newell, Phys. Rev. Lett. **73**, 2978 (1994).
[17] J. Lega, J. V. Moloney, and A. C. Newell, Physica D **83**, 478 (1995).
[18] A. Barsella, C. Lepers, M. Taki, and P. Glorieux, J. Opt. B: Quantum Semiclassical Opt. **1**, 64 (1999).
[19] J.-F. Mercier and J. V. Moloney, Phys. Rev. E **66**, 036221 (2002).
[20] L. M. Narducci and N. B. Abraham, *Laser Physics and Laser Instabilities* (World Scientific Publishing, Singapore, 1988).
[21] S. Longhi and A. Geraci, Phys. Rev. A **54**, 4581 (1996).
[22] M. Santagiustina, E. Hernández-Garcia, M. San-Miguel, A. J. Scroggie, and G.-L. Oppo, Phys. Rev. E **65**, 036610 (1 2002).
[23] M. Cross and P. Hohenberg, Rev. Mod. Phys. **65**, 851 (1993).
[24] A. C. Newell and J. V. Moloney, *Nonlinear Optics* (Addison Wesley Publishing Co., Reading, MA, 1992).
[25] Q. Feng, J. V. Moloney, and A. C. Newell, Phys. Rev. Lett. **71**, 1705 (1993).
[26] I. Aranson and L. Tsimring, Phys. Rev. Lett. **75**, 3273 (1995).
[27] C. Martel and J. Vega, Nonlinearity **9**, 1129 (1996).
[28] J. Vega, E. Knobloch, and C. Martel, Physica D **154**, 313 (2001).
[29] C. Bendr and S. A. Orszag, *Advanced Mathematical Methods for Scientists and Engineers* (McGraw-Hill, New York, 1978).
[30] J. Kevorkian and J. Cole, *Perturbation Methods in Applied Mathematics* (Springer-Verlag, Berlin, 1981).
[31] H. Chat and P. Manneville, Physica A **224**, 348 (1996).
[32] I. Aranson and L. Kramer, Rev. Mod. Phys. **74**, 99 (2002).
[33] D. Hochheiser, J. V. Moloney, and J. Lega, Phys. Rev. A **55**, R4011 (1997).
[34] I. Aranson, D. Hochheiser, and J. V. Moloney, Phys. Rev. A **55**, 3173 (1997).